Soil Dynamics and Earthquake Engineering 115 (2018) 90–103

Contents lists available at ScienceDirect

Soil Dynamics and Earthquake Engineering

journal homepage: www.elsevier.com/locate/soildyn

Dynamic response of monopiles in sand using centrifuge modelling

Marcos Massao Futai[a,*], Jing Dong[b], Stuart K. Haigh[c], S.P. Gopal Madabhushi[c]

[a] Department of Structural and Geotechnical Engineering, School of Engineering, University of Sao Paulo, Av. Prof. Luciano Gualberto, travessa 3 n° 380, CEP 05508-010 São Paulo, SP, Brazil

[b] Country Garden, 19 F, Building 11, Nuode Zhong Xin, Fengtai District, Beijing, China

[c] Department of Engineering, University of Cambridge, Cambridge CB2 1PZ, United Kingdom

ARTICLE INFO

Keywords:
Centrifuge modelling
Wind turbine foundation
Monopile
Natural frequency

ABSTRACT

Monopiles are one of the most commonly used offshore foundation for wind turbines. Their static capacity, p-y curve and cyclic loading behaviour have been studied using 1 g tests and centrifuge tests, but there is little experimental data regarding their natural frequency, especially using centrifuge testing. The design of offshore wind turbine foundations is largely governed by natural frequency as resonance due to cyclic loading can cause damage and even failure. Understanding the dynamic response of the monopile under free vibration is thus critical to design. This paper presents the results of novel monopile (large diameter) and single pile (small diameter) tests in a centrifuge to for the first time directly determine the natural frequency (f_n) of the pile-soil system. An experimental methodology was used to define the natural frequency via measured acceleration and force time histories and their fast Fourier transforms (FFT) under a force applied at a controlled frequency. The effects of pile diameter, embedded length, free length of the tower and soil density on f_n were investigated in the centrifuge tests. The same models used in the centrifuge test at 50 g were also tested at 1 g in order to assess the relevance of earlier 1 g investigations into system behaviour. The measured natural frequency of wind turbine monopiles in centrifuge models during harmonic loading from a piezo-actuator, confirmed that soil structure interaction at an appropriate stress level must be taken into account to obtain the correct natural frequency. The experimental data was compared to theoretical solutions, giving important insights into the behaviour of these systems.

1. Introduction

Wind energy is becoming increasingly more attractive as a source of renewable energy and has widespread potential for application in different regions of the world. Wind turbine technology has been continuously improving, particularly with respect to mechanical and electrical innovations, leading to progressively larger and more powerful turbines And consequently tower heights have increased. This trend looks set to continue, with Wiser et al. [3] suggesting that the hub height will reach 160 m by 2030. In this scenario, the dynamic response of the tower and foundation will be of the utmost importance. The European Offshore Wind Energy Association [4] reported that 3018 MW of offshore wind energy was installed in European waters in 2015. By 2016, Europe had 81 wind farms with 3589 turbines and the cumulative installed capacity reached 12,631 MW. Although the majority of wind turbine capacity is being built in Europe, America and China have also established targets to develop 3305 MW and 10,000 MW of offshore wind energy by 2020 respectively [5]. Offshore wind turbines will hence play a significant role in the global electricity market in the future.

Currently monopiles account for 80% of offshore wind turbine foundations with gravity bases accounting for 9% [4]. The remaining foundations include jackets, tripods, tri-piles and floating foundations. The monopile is a short and rigid circular steel pipe pile, which has a slenderness ratio of approximately 5 [6]. It is a common foundation design for offshore wind turbines because it is economical at shallow water depths (10–25 m). The typical dimensions of a monopile are a 3–6 m outer diameter and 22–40 m length [7]. Although a monopile is a simple foundation design concept, understanding the dynamic soil-structure interaction (SSI) of a wind turbine on a monopile foundation is a complex task [6].

Offshore wind turbines (OWTs) experience high lateral loading and

Abbreviations: FFT, fast Fourier transform; MEMS, micro-electrical-mechanical system; OWT, offshore wind turbine; SSI, soil-structure interaction

* Correspondence to: Graduate Program of Civil Engineering, Structural and Geotechnical Engineering Department, Engineering School, University of São Paulo, Av. Prof. Luciano Gualberto, travessa 3 n° 380, CEP 05508-010 São Paulo, SP, Brazil.

E-mail addresses: futai@usp.br (M.M. Futai), jing.dong@cantab.net (J. Dong), skh20@cam.ac.uk (S.K. Haigh), mspg1@cam.ac.uk (S.P.G. Madabhushi).

https://doi.org/10.1016/j.soildyn.2018.08.007
Received 10 September 2017; Received in revised form 31 July 2018; Accepted 2 August 2018

Nomenclature

a and b	empirical parameters to calculate C_R and C_L, respectively
$A(\gamma)$ and $m(\gamma)$	strain-dependent parameters for G_{max} calculation
C_R and C_L	factors that account for the flexibility provided by the pile [1]
D	pile diameter
D_{10}	particle-size diameter for which 10% of the sand by mass was finer
D_{50}	particle-size diameter for which 50% of the sand by mass was finer
Dr	relative density
e	void ratio
E_o	elastic modulus at a depth of one pile diameter
E_{pe}	equivalent elastic modulus of pile
e_{max}	maximum void ratio
e_{min}	minimum void ratio
$f(\nu)$	Poisson's ratio effects as presented by Randolph [2]
F_h	horizontal force
f_n	natural frequency or measured natural frequency
$f_{n\text{-}str}$	natural frequency calculated as a fixed base or cantilever beam
$f_{n\text{-}TSSI}$	theoretical natural frequency considering SSI
G_{max}	small strain shear modulus
Gs	specific gravity of soil particles
L_P	embedded length of pile
I	moment of inertia
K	constant that depends on the soil's relative density
K_h	horizontal pile stiffness
K_{hr} or K_{rh}	coupling between horizontal and rotational pile stiffness
K_r	rotational pile stiffness
K_{str}	structural stiffness of the tower
L	free length.
L_T	free length of structure (single pile or monopile).
L_{Teq}	equivalent length
m	lumped mass on top of the tower
M	moment
n	gradient of elastic modulus referent, a linear variation with depth
N	scale factor of centrifuge modelling
p'	mean principal effective stress
PL	monopile
PS	single pile
t	wall thickness of monopile
u	horizontal displacement
η_L, η_{LR} and η_R	non-dimensional lateral, cross-coupling and rotational stiffness values, respectively.
β	parameter regarding SSI in the theoretical natural frequency
γ	shear strain
γ_d	dry soil unit weight
θ	rotation angle

a large moment at the seabed in comparison to the vertical loading. Byrne and Houlsby [8] stated that for a typical 3.5–5 MW turbine, the horizontal load from combined wind and wave loads is 4–6 MN, whereas the vertical loading is 6–10 MN. The wind and wave loads are cyclic in nature; thus a combination of extreme sea and wind states have to be taken into account. According to Byrne and Houlsby [8], on a hub that is 90 m above the sea floor, the maximum operational wind load would be approximately 1 MN and wave and current loads acting below the water surface level are approximately 1 ± 2 MN, thus producing a net lateral load of 2 ± 2 MN and a resulting moment of 200 ± 20 MNm. For design purposes, Arany et al. [9] developed a framework to calculate appropriate loading values based on a variety of turbine and environmental parameters. OWTs are dynamically sensitive structures because of their slender structural nature and the applied cyclic loads. The excitation frequency of offshore wind turbines should hence be carefully considered during the design phase to prevent resonance.

Fig. 1 illustrates the excitation frequencies of a typical wind turbine system as presented by LeBlanc [10]. The system is excited by the applied loading from wind and waves, but also by loading from the aerodynamic changes occurring during rotation of the blades. The frequency of rotational loading is termed the 1 P frequency, with the blade-passing frequency being to three times the rotational frequency of the turbine (3 P). The wind gust frequency is typically less than 0.1 Hz, whereas the frequency of high-energy wave loading ranges from 0.05 to 0.5 Hz [11].

During design, the selected system natural frequency needs to lie outside these excitation frequencies in order to avoid resonance and to reduce fatigue damage. Therefore, to ensure that the first natural frequency (f_n) of the system is consistent with all of these excitation frequencies, three options can be considered in the design phase: 'soft-soft', 'soft-stiff' or 'stiff-stiff' design, as shown in Fig. 1. To avoid resonance, f_n needs to be kept 10% away from both the 1 P frequency and 3 P frequency [12]. As shown in Fig. 1, for a soft-stiff system, f_n needs to be fitted in a very narrow band; thus, changes in the foundation stiffness due to cyclic loading may result in f_n entering either the 1 P frequency or 3 P frequency ranges. Although a soft-stiff design is the most cost effective and practical, the foundation stiffness and changes in the foundation stiffness due to cyclic loading need to be carefully determined to avoid resonance during the long design life of the structure.

To understand the dynamic response of the monopile foundation, Zaaijer [13] developed a dynamic model to predict the natural frequency of offshore wind turbine foundations and studied how sensitive the natural frequency is to the input parameters. Alexander [14] estimated the nonlinear resonant frequency of a single pile in nonlinear soil by determining analytical expressions for the natural frequency of the fundamental mode of a pile and Arany et al. [15] presented a methodology to calculate the natural frequency of an offshore wind turbine structure on a flexible foundation using Euler-Bernoulli beam theory and a three-spring model. Bhattacharya et al. [16] experimentally conducted a series of 1:100 scale 1 g model tests of a V120 Vestas turbine supported on monopiles and tetrapod suction caissons in kaolin clay and sand and Prendergast et al. [17] developed an experimental program to examine the effect of scour on the natural frequency of a scale-model monopile at a dense sand test site. Although small-scale tests on the natural frequencies of pile-soil systems have been conducted by Bhattacharya et al. [16] and Prendergast et al. [17], these tests were conducted at 1 g with a stress-state within the soil substantially different from that for a full-size foundation. As soil is a very non-linear material, the effects of this incorrect stress state on the system natural frequency is not easily quantified.

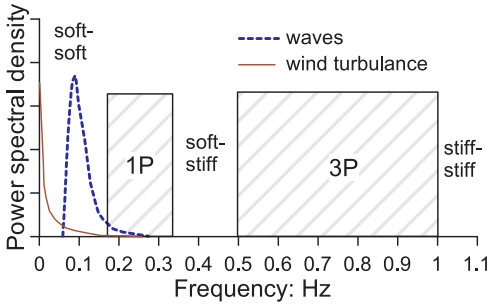

Fig. 1. Excitation frequencies acting on a typical wind turbine system (Leblanc, 2009).

The objective of this study is to use centrifuge models to aid in understanding of the dynamic response of pile-supported wind turbine structures. Well-characterised sand subjected to rigorous sample preparation was used to conduct the centrifuge tests with a dynamic actuator being used to apply low amplitude cyclic loading at varying frequency with the acceleration response of the pile foundation being measured. The experimental procedure enabled the natural frequency of the piles to be defined. Different diameters, embedded depths, free lengths and sand relative densities were used in the tests. The prototype model represents simple structures compare to real offshore wind structures, however, this condition reduces the uncertainties and allows to calibrate theoretical models with more clarity.

The literature results indicated that the majority of previous studies have been conducted using 1 g small-scale models. The PISA project (PIle Soil Analysis) employed field testing and computational modelling and this research represent an important advance because it associated field test of monopile, laboratory and site investigations, numerical simulation and calibration of design model [18].

This paper presents the results of centrifuge tests, which will be used not only to understand the prototype behaviour under free vibration but also to discuss the applicability of the small-scale models and simple theoretical solution.

2. Experimental setup

The soil used in the centrifuge tests was Hostun sand, acquired from the area of Drôme in the southeast of France. This sand has been regularly used in centrifuge tests at the Schofield Centre of the University of Cambridge [19–22] and in several other European centres. The sand contains a high percentage of silica ($SiO_2 > 98\%$) and has a grain shape varying from angular to sub-angular. The principal properties of this sand are summarized in Table 1.

An automatic sand pourer designed by Madabhushi et al. [23] was used to accurately prepare the sand in a tub. The relative densities of sand used in the tests were 35% (loose sand) and 70% (dense sand). Table 2 presents the properties of the sand samples used in this work.

The stiffness of the soil was determined during the centrifuge test via the shear wave velocity (Table 2), measured using a miniature air hammer as described by Ghosh & Madabhushi [24]. Five accelerometers were installed at different depths in a vertical array during pouring of the sand. The miniature air hammer was installed directly below all accelerometers. The shear wave velocity was obtained by measuring the wave travel time between two consecutive accelerometers using cross-correlation. The air hammer tests were performed at three different gravity levels (1 g, 30 g, and 50 g) for loose sand and at four different levels (1 g, 10 g, 30 g, and 50 g) for dense sand. As centrifuge modelling results in homologous stress fields between model and prototype and hence identical soil stiffness, the shear wave velocities measured in the model are the same as those for the prototype; however, the depth in the prototype is N times larger. N is the scaling factor and the scaling law of others parameters are shown in Table 3. Details of principles of centrifuge modelling and scaling law can be seen in Madabhushi [25].

The model monopiles were fabricated from lengths of aluminium tube and the single piles were made using a solid cylindrical aluminium rod. Four monopile (PL) and four single pile (PS) models were used in each centrifuge test, the dimensions of these models and the prototypes are shown in Table 4. The flexural rigidities were 2.208 kN m^2 and 0.088 kN m^2 for the monopile and single pile respectively at model scale, representing values N^4 times greater at prototype scale (Table 3) and thus corresponding to 1.38×10^7 kN m^2 and 5.51×10^5 kN m^2 for the monopile and single pile respectively.

Tests were conducted in the Turner beam centrifuge at the Schofield Centre, Cambridge University [26]. The details of the prototype models are presented in Table 4. The centrifuge experiments were divided into sixteen flights (eight for each sand density) to study the dynamic behaviour of each of the pile foundations. The program was conducted in an 850 mm diameter tub at 50 g. The monopile wall thickness at prototype scale is 85.5 mm.

The test model used in the current study was based on the dimensions of a typical 3.5 MW offshore wind turbine, as shown in Fig. 2. The horizontal and moment loads acting on the turbine could be represented simply by a single horizontal load acting 30 m above the mudline [9]. As a typical monopile is 4 m in diameter, driven 20 m into the seabed with a wall thickness of 150 mm a simplified prototype that is 50 m in height with a lumped mass on the top can represent a real monopile foundation.

Owing to size limitations this could not be modelled at full-scale in this project and instead a prototype 50% of the size in all dimensions was modelled. The prototype thus represents a 1:2 scale model of a monopile foundation for a 3.5 MW offshore wind turbine. Using PL4 as an example, the scaled model is 500 mm in height and 38 mm in diameter, with a 1.71 mm wall thickness. The total mass is 0.76 kg, including the 0.29 kg monopile mass and a 0.54 kg lumped mass at the pile head. The lumped mass was fixed on the top of the monopile and contained the piezo-actuator (Fig. 3b). PL1 to PL3 are scale models similar to PL4, whereas PS1 to PS4 simply decrease the diameter to investigate parametric effects.

The piles were tested by applying a cyclic force at a given frequency at the top of the structure using a dynamic piezo-actuator. The dynamic actuator, developed by Cedrat Technologies [27], comprises a piezoelectric device (APA400MML) that converts an electrical input to extension of a stack of piezo-crystals. In this paper, a system similar to that of Cabrera et al. [28] was produced with some adaptations. The piezo-actuator was attached between the top of the structure and a moving counterweight, held in a linear bearing, to enable the extension of the actuator to produce a cyclic force on the top of the pile. The piezoelectric device is fixed on one side to the pile head and on the other side pushes a reaction mass. The dynamic actuator transforms an electrical input into a mechanical action of the same frequency that is transferred to the structure [26].

As shown in Fig. 3, the piezo-actuator on the top of the monopile vibrated horizontally. Through adjusting the frequency provided by a function generator, the vibrating frequency could be changed. The dynamic response of the pile could thus be recorded by three MEMS (micro-electrical-mechanical system) accelerometers M1 to M3 attached to the outer wall of monopile with a load cell fixed next to the piezo-actuator on the top plate recording the input excitation. The position of the MEMS is shown in Fig. 3a.

The typical test layout is shown in Fig. 3c. The piles were driven under 1 g conditions by hand using a rubber hammer. While this will have some impact on the disturbance of soil around the pile relative to a pile installed with the full-scale stresses acting on the soil, this simplification was made in order to ensure complete decoupling of the final pile from any driving system which might affect its behaviour. Once the centrifuge had been accelerated to 50 g, different frequency sinusoidal motions and square motions were applied on the top of the pile through the piezo-actuator. The frequency range used was limited to a maximum of 600 Hz in order to avoid the resonant frequency of the piezo-actuator at 634 Hz [27]. This process was repeated for each pile.

Table 1
Geotechnical properties of Hostun sand [20].

Property	Value
D_{10}	0.286 mm
D_{50}	0.424 mm
e_{min}	0.555
e_{max}	1.010
G_s	2.65
ϕ_{crit}	33°

Table 2
The physical properties of sand samples.

Property	Loose	Dense
e	0.85	0.69
γ_d (kN/m^3)	14.45	16.65
Dr (%)	35	70
Vs* (m/s)	90	115
Vs** (m/s)	250	280

* at 0.2 m depth tested at 1 g.
** at 10 m of depth (prototype scale) tested at 50 g.

Table 3
Centrifuge scaling laws.

Parameter	Model/ prototype	Dimensions	Units
Acceleration	N	$L\,T^{-2}$	g (m/s^2)
Length	1/N	L	m
Area	1/N^2	L^2	m^2
Volume	1/N^3	L^3	m^3
Mass	1/N^3	M	Kg
Stress	1	$M\,L^{-1}\,T^{-2}$	N m^{-2}
Strain	1	–	–
Time (dynamic)	1/N	T	s
Frequency	N	T^{-1}	s^{-1}
Inertial Moment	1/N^4	L^4	m^4
Flexural rigidity	1/N^4	$M\,L^3T^{-2}$	N m^2

3. Measurement of soil stiffness and pile stiffness

Soil's small-strain shear modulus is an important parameter in SSI analysis. It is well known that the small strain shear modulus, G_{max}, depends on the effective stress and hence increases with depth. The measured variation of G_{max} with depth for the centrifuge model was compared with three empirical equations from the literature in order to investigate their veracity.

An equation for the variation of G_{max} with stress was proposed by researchers including Seed and Idriss [29] who proposed that:

$$G_{max} = 1000 \quad K p'^{0.5} \tag{1}$$

where K is a constant that depends on the soil relative density D_r, $K = 0.586 + 16.5D_r$ for $30\% \le D_r \le 90\%$, and p' is the mean principal effective stress.

Another well-known empirical relationship for G_{max} is given by Hardin and Drnevich [2], who proposed that:

$$G_{max} = 3230\frac{(2.973-e)^2}{1+e}p'^{0.5} \tag{2}$$

where e is the void ratio of sand.

Oztoprak and Bolton [30] also proposed an expression for the small-strain shear modulus adapted from that of Hardin and Black [31]:

$$G_{max} = \frac{A(\gamma)p_a}{(1+e)^3}\left(\frac{p'}{p_a}\right)^{m(\gamma)} \tag{3}$$

where $A(\gamma)$ and $m(\gamma)$ are strain-dependent parameters and p_a is a reference pressure of 100 kPa (atmospheric pressure). In this work, $\gamma = 0.001\%$ was adopted, corresponding to $A(\gamma) = 5760$ and $m(\gamma) = 0.49$.

The experimental G_{max} data were obtained from measured shear wave velocities which were assumed to be constant between a given pair of accelerometers. Fig. 4 presents the variation of G_{max} with prototype depth estimated from the empirical formulas and the measured experimental results. 5–12 determinations of G_{max} were performed, thereby enabling the mean value, as shown in Fig. 4.

It can be seen that while all three formula gave adequate predictions of shear stiffness variation, the formula proposed by Seed and Idriss [29] underestimated the results for loose sand whereas the formula proposed by Hardin and Drnevich [2] underestimated those for dense sand. The equation proposed by Oztoprak and Bolton [30] presented the best fit to the dataset (Fig. 4).

The dynamic stiffnesses of the foundations, considering SSI, have been determined using physical, discrete, continuous and numerical models. The foundation behaviour under combined loading can be assessed using the coupled spring model (Fig. 5d). The relation between the horizontal force (F_h) and horizontal displacement (u) and between moment (M) and rotation (θ) can be defined by the stiffness matrix:

$$\begin{Bmatrix} F_h \\ M \end{Bmatrix} = \begin{bmatrix} K_h & K_{hr} \\ K_{rh} & Kr \end{bmatrix} \begin{Bmatrix} u \\ \theta \end{Bmatrix} \tag{4}$$

where K_h, K_r and K_{hr} ($K_{hr} = K_{rh}$) are horizontal, rotational and coupling between horizontal and rotational stiffness, respectively.

Many combinations of springs can be used to represent the foundations. The idealized model for shallow foundations is straightforward, but for monopile foundations, it is not as simple. The first step in solving the problem is to define a stiffness matrix to calculate the monopile behaviour.

The stiffness of the foundation system depends on the stiffness of both the pile and the soil. The structural parameters can be precisely determined, but determining the soil-structure response under combined load is not as simple. The behaviour of the foundation system can be separated into rigid piles in which the pile is stiff relative to the surrounding soil and remains approximately straight and flexible piles which curve substantially under the applied loads.

Randolph [32], Novak and El Sharnouby [33] and Pender [1] proposed solutions for flexible piles whereas rigid pile solutions were presented by Carter and Kulhawy [34], Higgins et al. [35] and Arany et al. [36] for homogeneous soil and linear and nonlinear variations of G_{max} with depth, respectively. The characteristics of a monopile often lead to it being considered as a rigid pile.

The monopile and single small diameter pile tested in this paper

Table 4
Models of monopile and single pile and experimental program in prototype scale (50 g).

Pile and sand		Models (L_P, L_T, t in mm)				prototype scale (50 g) (L_P, L_T, t in m)						
Loose	Dense	$L_p + L_T$	D	t	EI (Nm^2)	D	L_P	L_T	t	EI (Nm^2)	L/D	H/D
PL-1L	PL1D	400	38	1.71	2208	1.9	10	10	0.086	1.38×10^{10}	5.26	5.26
PL-2L	PL2D	450	38	1.71	2208	1.9	12.5	10	0.086	1.38×10^{10}	5.26	6.58
PL-3L	PL3D	500	38	1.71	2208	1.9	15	10	0.086	1.38×10^{10}	5.26	7.89
PL-4L	PL4D	500	38	1.71	2208	1.9	10	15	0.086	1.38×10^{10}	7.89	5.26
PS-1L	PS1D	400	12.7		88	0.635	10	10	–	5.51×10^{8}	15.75	15.75
PS-2L	PS2D	450	12.7	–	88	0.635	12.5	10	–	5.51×10^{8}	15.75	19.69
PS-3L	PS3D	500	12.7	–	88	0.635	15	10	–	5.51×10^{8}	15.75	23.62
PS-4L	PS4D	500	12.7	–	88	0.635	10	15	–	5.51×10^{8}	23.62	15.75

L and D indicate loose and dense sands, respectively; $L_P + L_T$ – total length of pipe or bar; D is the pile diameter; L_P is the embedded depth; L_T is the free length; and t – wall thickness of monopile.

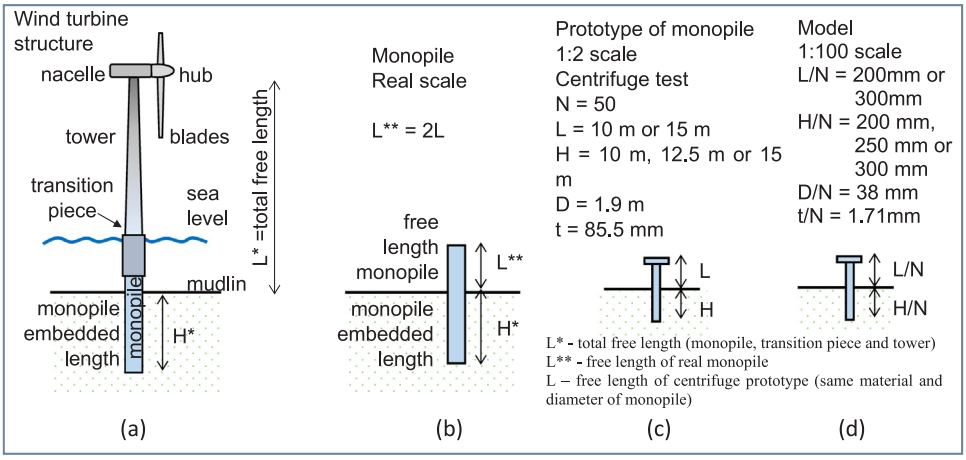

Fig. 2. Scale model: (a) OWT components, (b) monopile, (c) prototype of monopile and (d) model scale.

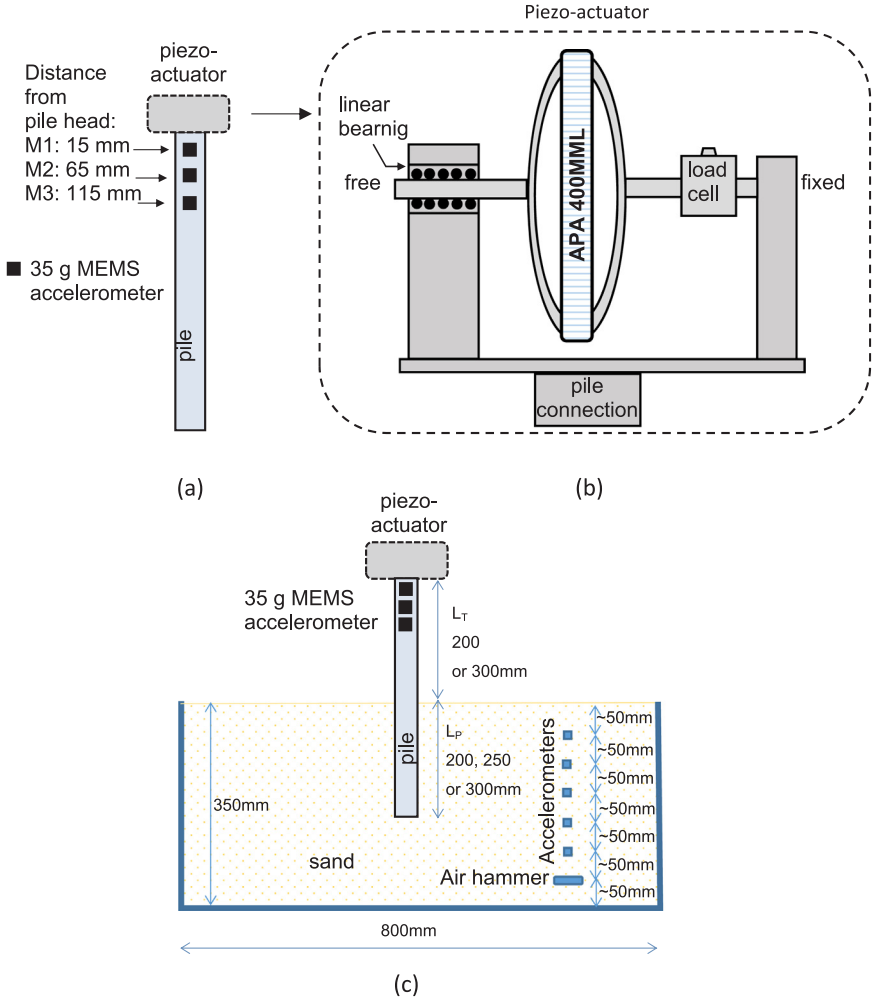

Fig. 3. Dynamic apparatus and pile instrumentation: (a) position of MEMS accelerometer and piezo-actuator, (b) details of piezo-actuator and (c) typical test layout.

present approximately rigid behaviour owing to their high bending stiffness with the shear modulus of the sand increasing nonlinearly with depth (Fig. 4). The expressions proposed by Higgins et al. [35] and Arany et al. [36] for pile stiffness were thus chosen, with the expressions being rearranged to introduce a function of the elastic modulus varying with depth:

$$\frac{E_{(z)}}{E_o} = \frac{z}{D} \tag{5}$$

$$\frac{E_{(z)}}{E_o} = \left(\frac{z}{D}\right)^{0.5} \tag{6}$$

In fact, the study of Higgins et al. [35] focused on defining the horizontal displacement and rotation of a rigid pile subjected to horizontal force and moment. The flexibility matrix of Higgins et al. [35]

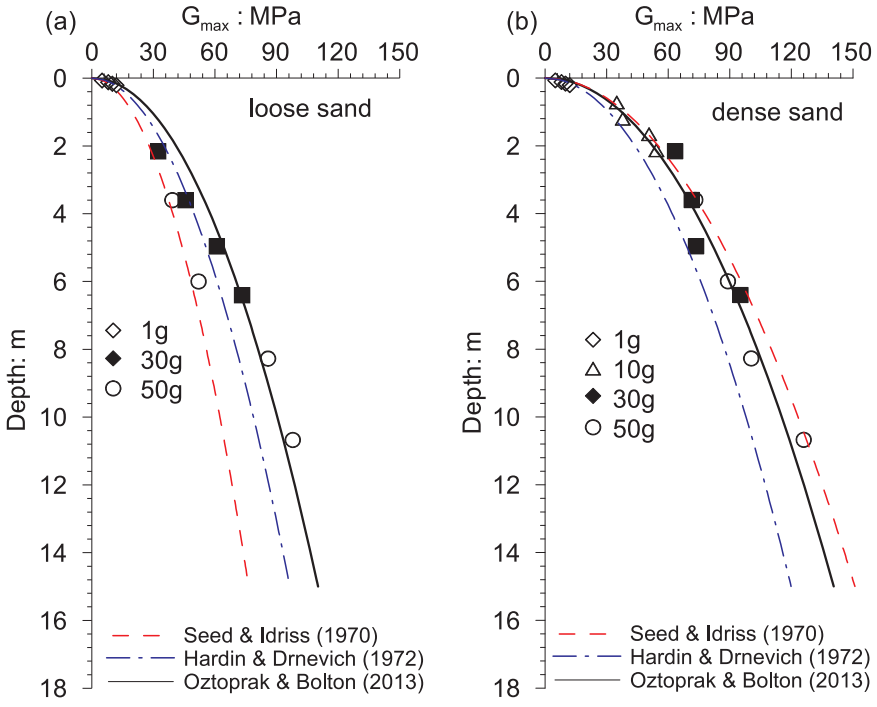

Fig. 4. Results of small-strain shear modulus for (a) loose sand and (b) dense sand.

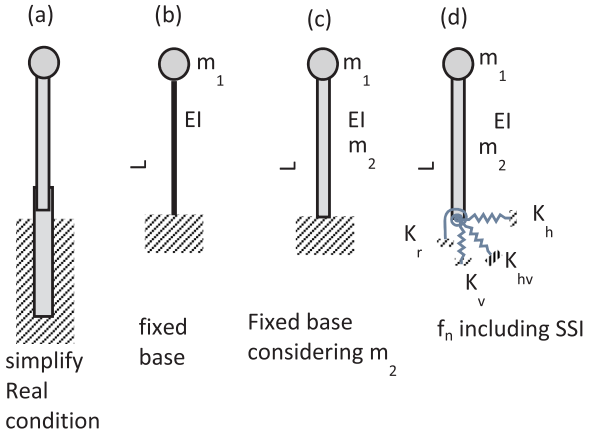

Fig. 5. Model idealizations for calculation of natural frequency.

was inverted by Arany et al. [36]. Tables 5, 6 summarizes the expressions and parameters that are needed to define the foundation stiffness. As these expressions are dimensionally inconsistent they are only valid in SI units.

The Poisson's ratio effects, $f_{(\nu)}$, can be calculated using Randolph [32], Shadlou and Battacharya [37] or Jalbi et al. [38]. The Randolph [32] recommendation for calculation of Poisson's ratio effects was adopted in this work.

As the soil stiffness varies nonlinearly with depth, different n values must be used for the Higgins et al. [35] expression for the 1 g small-scale tests and centrifuge tests. The Shadlou and Battacharya [37] expression conversely can use identical parameters as a parabolic expression fits all the soil stiffness data (Fig. 4). The parameters for equations (7) and (12) are presented in Table 7. The elastic modulus was calculated by elasticity theory using the experimental values of G_{max} (Fig. 4) and adopting a Poisson ratio equal to 0.3. Because the piles were tested under small amplitude vibration, the horizontal displacement and strain were very low and hence G_{max} values were used in the pile stiffness calculation. Shadlou and Bhattacharya [37] and Arany et al. [39] also considered the static and dynamic wind turbine structure stiffness are similar to calculate the natural frequency.

The coefficient of subgrade reaction, n_h, was determined by Vesic [40] propose using linear variation of elastic modulus fitted by data of Fig. 4 and the results are presented in Table 7.

The overall stiffness of a foundation comprising of a flexible pile depends on both the soil's shear modulus and the pile stiffness, however as the piles become rigid the effect of their stiffness on system response becomes negligible.

The dynamic behaviour of the wind turbine structure depends on the SSI. The simplified structural condition (Fig. 5a) was calculated as a fixed base or cantilever beam with mass m_1 concentrated on the free end (Fig. 5b), resulting in a natural frequency as given by Eq. (13).

$$f_{n-str} = \frac{1}{2\pi}\sqrt{\frac{3\ EI}{L_T^3\ m}} \tag{13}$$

It is possible to also consider the mass of the tower (or free length), m_2, as illustrated in Fig. 5c. The natural frequency can then be calculated using the van der Tempel and Molenaar [41] solution for the fixed based condition (Eq. (14)).

$$f_{n-str} = \frac{1}{2\pi}\sqrt{\frac{3.04\ \ EI}{L_T^3(m_1+0.227\ \ m_2)}} \tag{14}$$

The SSI can be taken into account using coupled springs (Fig. 5d). Normally, two or three springs in the linear regime are used. It is possible to summarize the solutions of natural frequency that consider the SSI, $f_{n\text{-}TSSI}$, as a fixed base natural frequency multiplied by a

Table 5
Impedance function.

Parameters	Rigid	Flexible
$\frac{K_h}{E_o r}=$	$\frac{a_1}{f_{(\nu)}}\left(\frac{L_P}{D}\right)^{a2}$ (7)	$a_1'\left(\frac{Epe}{E_o}\right)^{a_2'}$ (10)
$-\frac{K_{hr}}{E_o r^2}=$	$\frac{b_1}{f_{(\nu)}}\left(\frac{L_P}{D}\right)^{b2}$ (8)	$b_1'\left(\frac{Epe}{E_o}\right)^{b_2'}$ (11)
$\frac{K_r}{E_o r^3}=$	$\frac{c_1}{f_{(\nu)}}\left(\frac{L_P}{D}\right)^{c2}$ (9)	$c_1'\left(\frac{Epe}{E_o}\right)^{c_2'}$ (12)

Table 6
Parameters of Impedance function to be used in Table 5.

Parameter	Rigid		Flexible	
	[35]	[37]	[1]	[37]
a_1 or a_1'	4	5.33	1.7	2.03
a_2 or a_2'	1.66	1.07	0.29	0.27
b_1 or b_1'	6.7	7.2	0.96	1.17
b_2 or b_2'	2.6	2	0.53	0.52
c_1 or c_1'	15.4	13	1.2	1.42
c_2 or c_2'	3.45	3	0.77	0.76

Table 7
Elastic modulus parameters and coefficient of subgrade reaction for loose and dense sand.

Sand/ Pile	E_{pe}/E_o		n_h (MN/m^3)	
	1 g	50 g	1 g	50 g
Loose -PS	69967	10283	100	25
Loose-PL	12830	1890	80	28
Dense-PS	51880	7599	200	30
Dense-PL	9467	1397	150	40

constant β (Eq. (15)).

$$f_{n-TSSI} = \beta f_{n-str} \quad (15)$$

β gives the ratio between the natural frequency with SSI, and that for the fixed base system. Owing to the increased flexibility of the system due to the soil, the value of β ≤ 1. Analytical solutions for β depend on the theoretical solution and hypotheses adopted. Several solutions were selected for comparison with the experimental results as presented in Table 8.

Darvishi-Alamouti et al. [42] deduced other formulae to estimate the structure's first natural frequency. This used the principle of conservation of energy (Rayleigh method). Unlike other equations, Darvishi-Alamouti et al. [42] used the concept of a beam on an elastic foundation to model the deep foundation and assumed that the modulus of subgrade reaction increases linearly with depth (coefficient of subgrade reaction, n_h). The stiffness correction factor (γ_k) and the mass correction factor (γ_m) for rigid or flexible piles can be found in Darvishi-Alamouti et al. [42]. Eq. (17) to (20) can be used for any structure represented by simple impedance function, including for a pile under horizontal loading to determine the natural frequency.

Equations (16) to (18) were developed for seismic applications and equations (19) and (20) were deduced specifically for wind turbine structures. The amplitude of vibration is very different from seismic application because the amplitude of vibration of a wind turbine is very small. The adequate selection of impedance function permits a convenient application of the equations in Table 8.

where:

$$K_{str} = \frac{3\ EI}{{L_T}^3} \quad (21)$$

C_R and C_L are factors that account for the flexibility provided by the pile [36]

γ_k is the stiffness correction factor for rigid or flexible piles [42].

γ_m is the mass correction factor for rigid or flexible piles [42].

4. Dynamic response of monopiles

During centrifuge testing the pile foundations were vibrated by the piezo-actuator at frequencies between 30 and 500 Hz in model scale. Using the centrifuge scaling laws (Table 3), the accelerations and frequencies in the model are N times greater than those for the prototype system while the force is N^2 times smaller [25]. The frequency range is thus 0.6–10 Hz at prototype scale. During each test, data is acquired from three MEMS accelerometers at different heights on the tower and the load cell measuring applied force (Fig. 3). Approximately 50 tests were performed for each pile, as an example data from test PL1D with excitation at 100 Hz (confirmed by FFT analysis) is shown in Fig. 6. The peak values of acceleration and applied force were obtained for each test. Low frequency (1 Hz, 2 Hz, 5 Hz and 10 Hz) square waves were also applied to the pile in order to investigate the frequency of free vibration of the system by taking the FFT of the acceleration response after each step in force. The 2 Hz square frequency was found to be best for defining the natural frequency because the higher frequency interfered with the free vibration while 1 Hz did not provide sufficient amplitude to vibrate the pile. Fig. 7 shows the response measured during test PL1D at model scale when subjected to a square wave with a frequency of 2 Hz.

The peak values of acceleration and force are plotted as a function of frequency, as shown in Fig. 8 for test PL1D (in model scale). The dynamic response of the structure results in increased accelerations due to resonance when the vibration is close to the system's natural frequency. It is possible to observe that the three MEMS (Fig. 8a) indicate the same peak response (101.1 Hz in model scale) however the applied force also shows a peak at this frequency. In order to calculate the resonant frequency, the acceleration response should be normalized by the applied force, giving the results shown in Fig. 8c. It can be seen that the peak response, i.e. resonance, occurs at 98.2 Hz. The square wave excitation (Fig. 7) was also analysed using FFTs, giving the results shown in Fig. 8. The first peak of the power spectral density is the natural frequency (106 Hz in the model or 2.1 Hz in the prototype). The normalized data (Fig. 8c) does not show the second peak that was seen for acceleration (Fig. 8a) or force (Fig. 8b), as this is merely an artefact of the actuator system, representing the actuator's natural frequency. This result confirms that the first peak is the pile-soil natural frequency of the system.

The same procedure and results for acceleration and FFT were followed for the monopiles, yielding the results summarized in Fig. 9 for loose and dense sands. The data of accelerations (Fig. 9) were normalized by the applied forces as shown in Fig. 10. There is only one peak in Fig. 10 corroborating that it is the natural frequency. Similar data were obtained for single piles (PS), with all the results of natural frequency in prototype scale being presented in Table 9.

5. Effects of dimensions of pile: diameter, embedded depth, and free length

The embedded depth of pile or L_P/D ratio changes the foundation stiffness as shown by the analytical expressions in Table 4. Consequently, it is expected that the system natural frequency will increase as the embedded length increases.

Fig. 11 shows the measured natural frequency of the piles with different embedded depths, 10 m, 12.5 m and 15 m at prototype scale.

Table 8
Values of β considering the soil structure interaction.

Reference	β
Veletsos and Meek [43]	$\frac{1}{\sqrt{1+\frac{K_{str}}{K_h}\left(1+\frac{K_h L^2}{K_r}\right)}}$ (16)
Gazetas [44]	$\frac{1}{\sqrt{1+\frac{K_{str}}{K_h}+\frac{K_{srt} L}{K_{hr}}+\frac{K_{srt} L^2}{K_r}}}$ (17)
Kumar and Prakash [45]	$\frac{1}{\sqrt{1+\frac{60}{H}\left(\frac{K_{str}}{K_h}+\frac{K_{str} L^2}{K_{hr}}\right)^{1.5}}}$ (18)
Arany et al. [36]	$C_R C_l$ (19)
Darvishi-Alamouti et al. [42]	$\sqrt{\frac{\gamma_k}{1+\gamma_m}}$ (20)

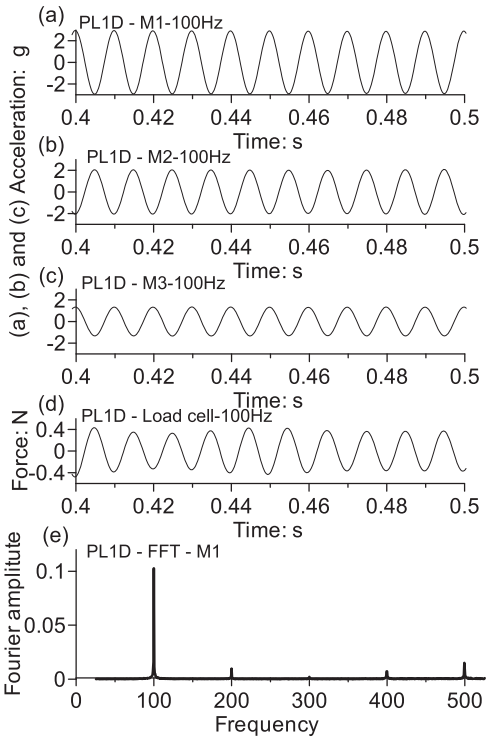

Fig. 6. Results of accelerations and force of PL1D monopile submitted to 100 Hz in model scale.

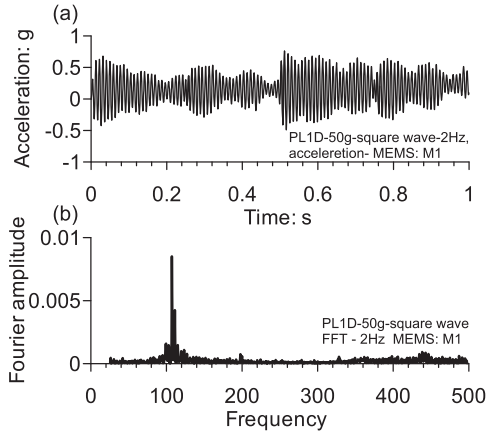

Fig. 7. Response to acceleration under square wave of 2 Hz of PL1D.

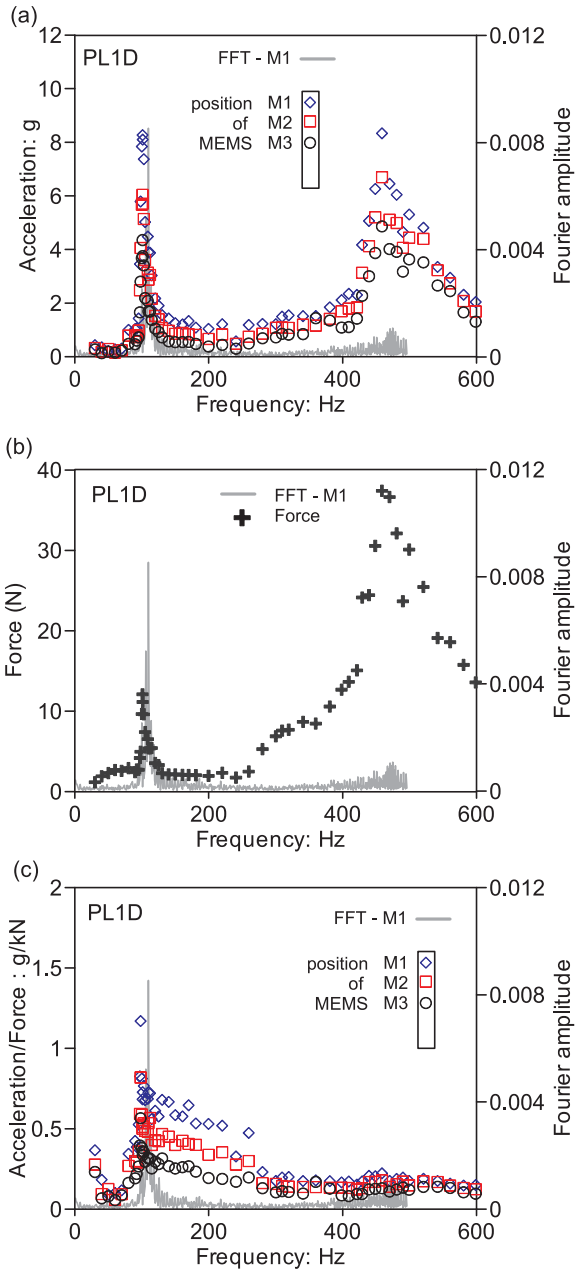

Fig. 8. Results of PL1D in model scale: (a) acceleration, (b) force response under forced frequency and (c) acceleration response normalized by the applied force.

The natural frequency increases as the pile embedded depth increases (or L_T/L_P decreases), but the changes are small (Table 7) This is probably due to monopiles of this length being effectively fixed at some depth less than the length of the pile itself. The f_n values of monopiles are higher than those of single piles and the f_n of piles installed in dense sand is higher than those installed in loose sand (Fig. 11a). Fig. 11b shows that single piles in dense sand suffer a smaller reduction in natural frequency relative to the fixed-base case than those in dense sand for any given embedment owing to the increased fixity provided by the denser sand. It can also be seen that for typical embedment ratios monopiles show a reduction in natural frequency by a factor of 2, whereas the single piles only reduce in natural frequency by a factor of approximately 1.5. As the monopiles have much higher stiffness than the single piles, the fixity stiffness required from the soil such that the system natural frequency reduces by a given factor is substantially higher than that for a single pile, hence requiring a substantially higher embedment. For a real structure, the dynamics of the tower structure and transition piece would also need to be considered along with that of the pile itself.

Using Fig. 11 to understand the contribution of diameter to f_n, it can be concluded that the diameter is more important than the L_T/L_P relation. Fig. 12 presents a comparison between the single pile and the monopiles under the same condition. It can be observed that the f_n of the single pile is 0.28 times that of the monopile. As the E, L_T and top head mass of both piles are the same, the theoretical relation between $f_{n\text{-}str}$ for the single pile and monopile can be obtained by Eq. (14) being the square root of value between the moments of inertia, in this case 0.20. The experimental value (0.28) is higher than theoretical one (0.20), as shown in Fig. 12, and this difference is due to soil-structural interaction.

The influence of free length can be analysed using tests P1 and P4 (Table 7). For example, in the results of PL1D and PL4D the increase of free length from 10 m to 15 m causes a decrease in the natural frequency from 2.022 Hz to 1.367 Hz. Thus, the 50% increase in the free

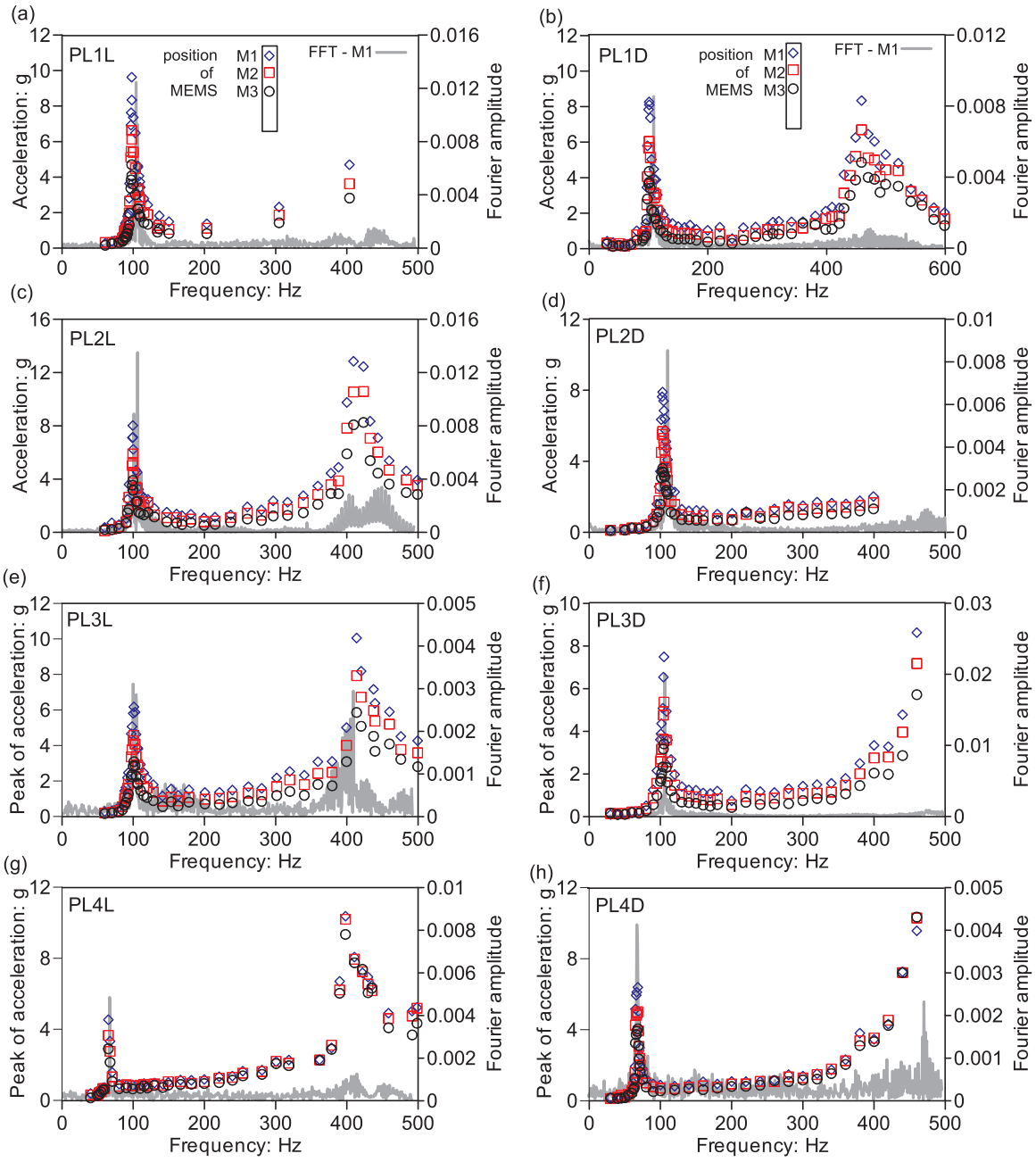

Fig. 9. Dynamic response of monopiles to define the natural frequency.

length causes practically the same reduction (48%) in the natural frequency. This result is similar to the other piles, as shown in Fig. 13. The f_n of the 15 m embedded depth is 0.67 times that for L_T = 10 m (specifically for this experimental result). The theoretical ratio between fixed base (Eq. (14)) natural frequencies is 0.54, lower than that found experimentally experimental data (0.67). The relation of free length cannot be considered without the soil-structure interaction. Superficially it may be concluded that the free length (Fig. 13) is more important than the embedded depth (Fig. 11). However, this depends on the SSI or pile stiffness. The free length influences the $f_{n\text{-}str}$ calculation (Eq. (15)) together with the pile diameter (EI/L_T^3), and the embedded depth influences the β value (Table 6).

6. Influence of soil density on pile response

Piles PL1L to PS4L were installed in loose sand, and piles PL1D to PS4D were installed in dense sand (Table 7). The influence of sand density on natural frequency was found to be small. Fig. 14 presents a comparison of the natural frequency of single piles and monopiles in loose and dense sands. The f_n of piles installed in dense sand is only 4% higher than that of piles installed loose sand (Fig. 14), even though the relative density has been doubled. The lower difference occurred because the range and the minimum value of embedded depth did not considerably change the soil-pile stiffness (Table 4) or β parameter (Table 6).

7. Comparison to 1 g tests

The monopiles and single piles were also tested under 1 g conditions. The same methodology, models (dimensions), instrumentation, piezo-actuator and L_T/L_P ratio were used to conduct the 1 g tests. Fig. 15a shows an example of the results, Fig. 15b and c being included

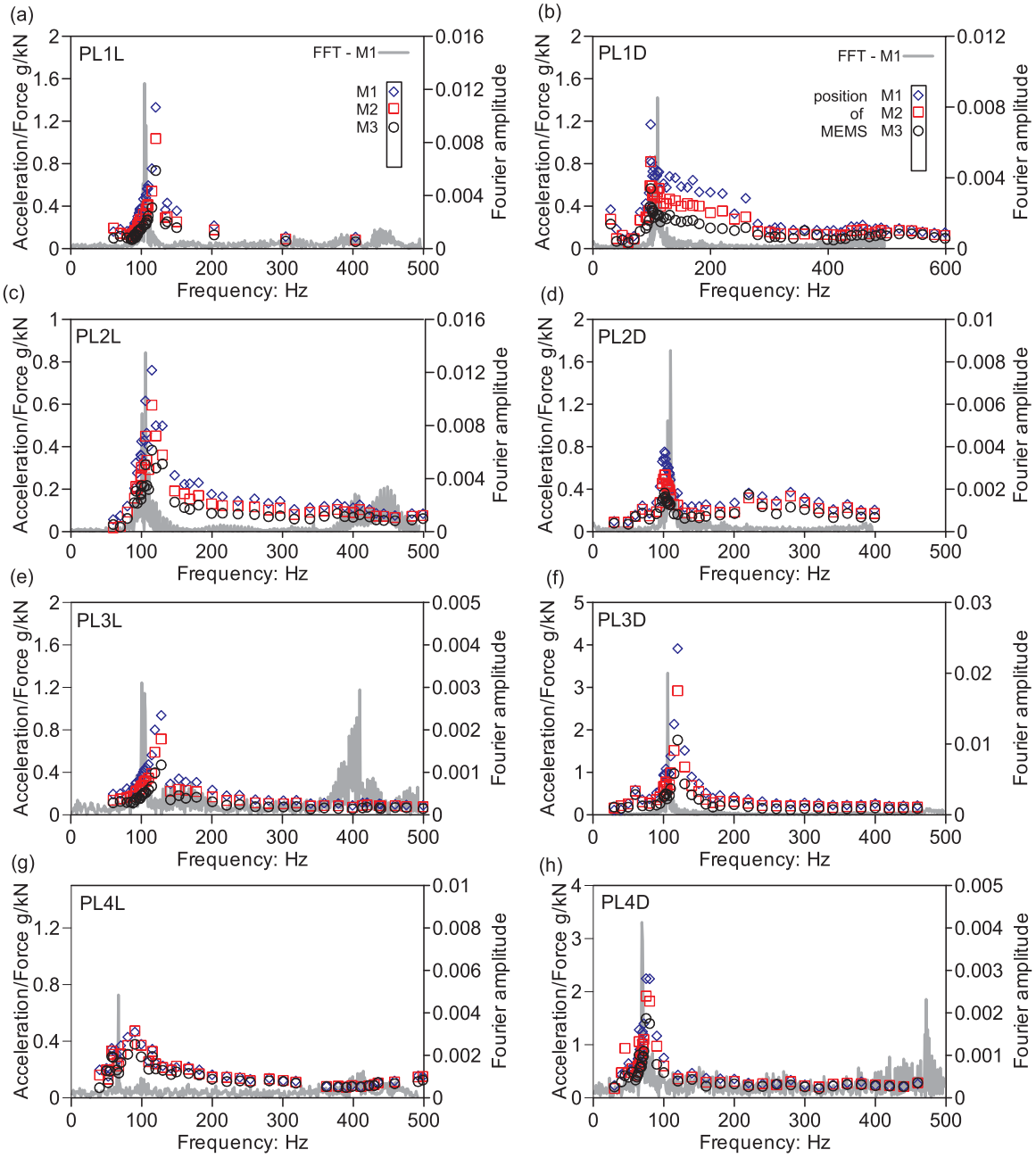

Fig. 10. Acceleration response normalized by the applied force.

Table 9
Results of natural frequency in prototype scale.

Loose sand		Dense sand	
Test	f_n (Hz)	Test	f_n (Hz)
PL1L	1.957	PL1D	2.022
PL2L	1.990	PL2D	2.062
PL3L	2.020	PL3D	2.100
PL4L	1.300	PL4D	1.367
PS1L	0.540	PS1D	0.563
PS2L	0.550	PS2D	0.579
PS3L	0.575	PS3D	0.600
PS4L	0.325	PS4D	0.363

to compare the results to those of the centrifuge test and fixed base test, respectively. The model scale natural frequencies of all centrifuge tests were higher than those of the 1 g tests and lower than the fixed base frequency. This is as expected owing to the lower fixity provided by the sand at 1 g by virtue of its lower effective stress and hence stiffness. The ratio between the natural frequencies measured at Ng and at 1 g for PL1L, for example, is 1.7 for a g-level of 50 g. The results indicate that the very low confining stresses in the 1 g model tests are not representative of the behaviour at more realistic stress level as indicated by the centrifuge tests. While the structural stiffness of the model pile is independent of stress level, the foundation stiffness substantially increases with increasing stress level owing to increasing soil confinement. Because both of these stiffnesses affect the system's natural frequency, no simple unique scaling law can be used to account for this complex relationship between the stiffnesses at 1 g and Ng.

The relation between the measured 50 g and 1 g natural frequencies in model scale is presented in Fig. 16. This ratio is always greater than

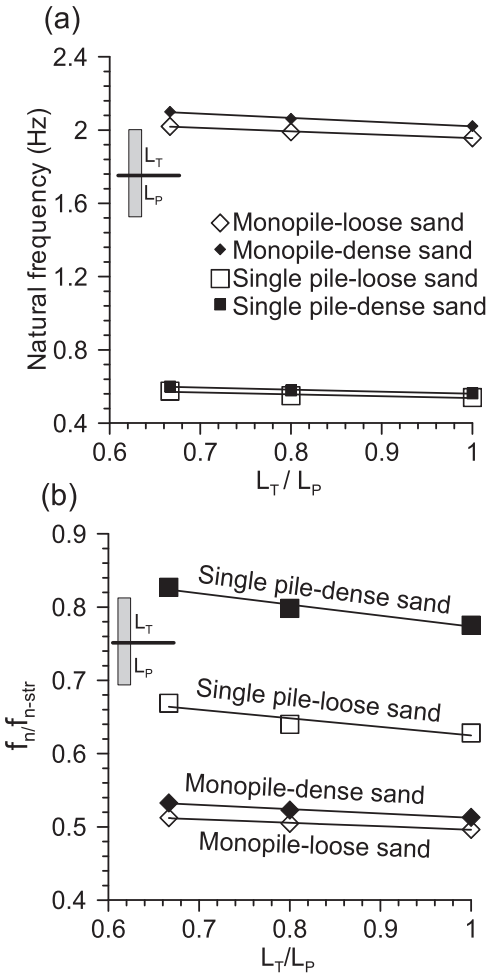

Fig. 11. Effect of embedded depth, L/H, on (a) natural frequency and (b) normalized frequency, $f_n/f_{n\text{-}f}$.

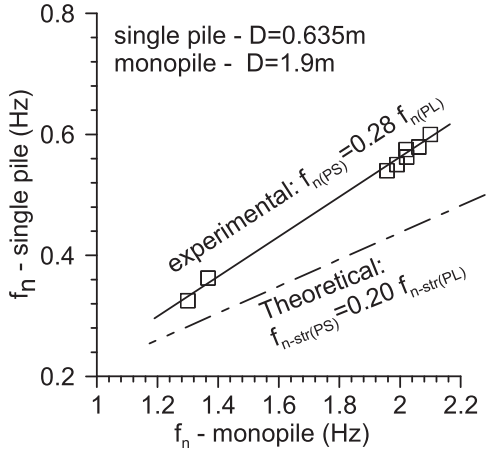

Fig. 12. Effect of diameter.

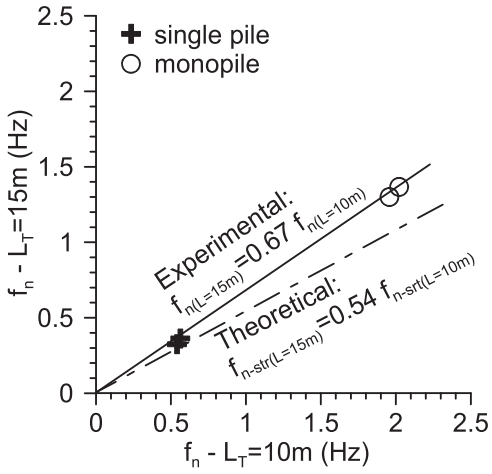

Fig. 13. Effect of free length.

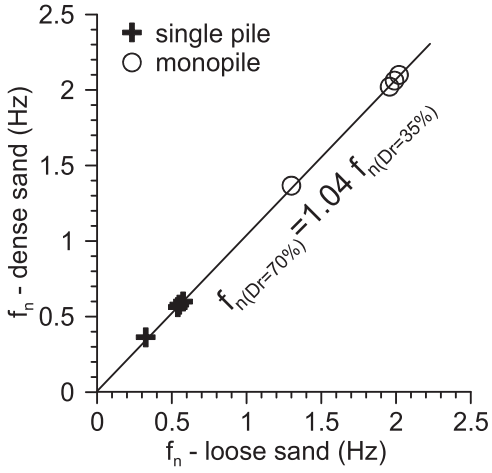

Fig. 14. Effect of sand density.

one, the average being 1.41. The single piles installed in loose sand showed the smallest ratio (mean value of 1.2), as shown in Fig. 16. The minimum ratio was 1.02 for PS4L, and the maximum 1.76 for PS1D (Fig. 16). The ratio for monopiles installed in loose sand (PLxL) was higher than that for monopiles installed in dense sand (PLxD), with the mean values being 1.55 and 1.46, respectively. However, the same analysis for the single pile provides the opposite result: the mean values being 1.20 for loose sand and 1.47 for dense sand. From the results, it is impossible to draw conclusions regarding the influence of relative density to define the prototype value of natural frequency based on the 1 g test. However, the small-scale model clearly produces higher values even when using a scaling law or dimensionless parameters.

The difference can be explained by considering both the SSI and the effective stress level. For the small-scale model, the effective stress is very low, and as is well known, the response of soil behaviour is non-linear, specifically the stress-strain curve or the small-strain shear modulus in this case. The theoretical ratio for G_{max} between prototype scale and the small-scale model is a constant that depends on the g-level, and in these cases, it is near $\sqrt{50}$. This ratio is independent of the embedded length of the pile and sand density. The G_{max} value directly influences the pile stiffness calculation equations (7) to (12) and consequently the $f_{n\text{-}TSSI}$ calculation (equation 16).

One way to understand the dynamic response of the small-scale 1 g and centrifuge tests is to calculate the equivalent free length of a fixed-base tower having the same natural frequency that was measured experimentally. This can be calculated using the measured natural frequency as $f_{n\text{-}str}$ in Eq. (14) and calculate the equivalent length (L_{Teq}). The results for the 1 g and centrifuge tests are shown in Fig. 17a and b, respectively, with the difference of equivalent length and free length ($L_{Teq} - L_T$) being normalized by the embedded depth (L_P).

The normalized equivalent length for the 1 g test varies between 0.35 and 1.3 with the average being 0.73 (Fig. 17a). For centrifuge test the normalized equivalent length was always lower than 0.6, the minimum value being 0.2 and the average 0.37 (Fig. 17b). The differences observed reflected the changes in pile fixity caused by the soil

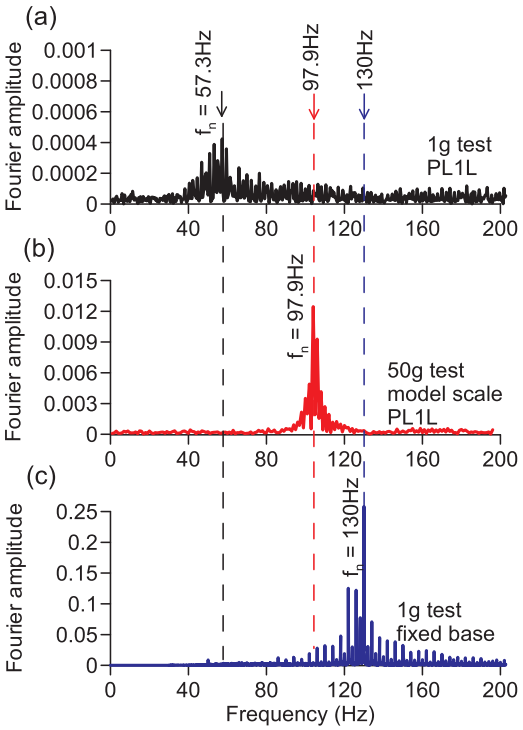

Fig. 15. Scale effect: the result of (a) PL1A in 1 g test, (b) PL1A in centrifuge test at 50 g in model scale and (c) test in fixed base condition in 1 g condition.

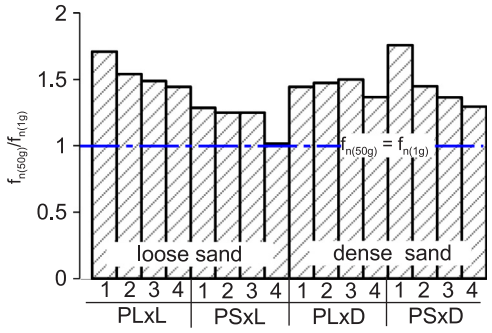

Fig. 16. Natural frequency ratio between 50 g test in the model and 1 g test.

stiffness. Owing to the very low confining stresses, a model tested at 1 g cannot be considered representative of a real deep foundation as the restraint applied to the pile is very low relative to the pile stiffness, resulting in the high observed normalized length of the foundation. The 1 g scale model thus cannot exactly represent the prototype behaviour even using a scaling law, though it may offer some indications of parametric effects.

8. Theoretical prediction and experimental data

The natural frequency of the system depends on the complex dynamic SSI occurring, but could be represented for design using springs representing the stiffness of the foundation. It is important for the soil stiffness to be well known, which is why the air hammer test was conducted in this study (Fig. 4). The theoretical value of f_n depends on the SSI idealisation, which can be performed using combinations of springs (Fig. 5d). Furthermore, the calculation of the theoretical f_n requires values for the foundation stiffness. In real conditions, the calculation of natural frequency has considerable uncertainty in all areas: the mathematical model, soil stiffness, and foundation stiffness.

Five analytical methods were selected to compare with the measured values: Veletsos and Meek [43], Gazetas [44], Kumar and Prakash [45], Arany et al. [36] and Darvishi-Alamouti et al. [42].

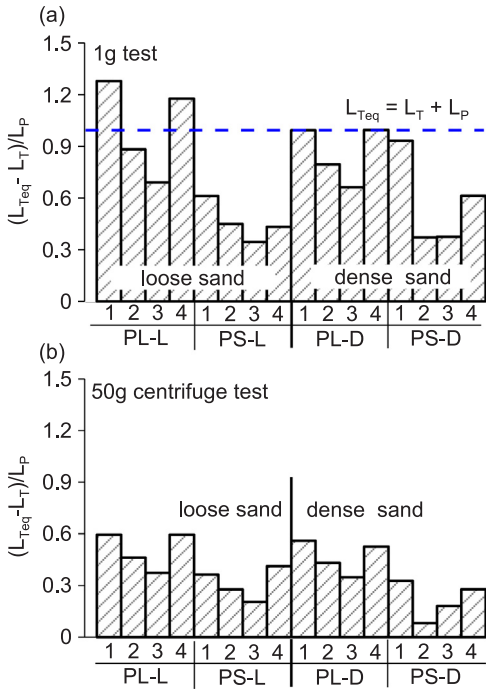

Fig. 17. Normalized equivalent length: (a) 1 g test and (b) 50 g centrifuge test.

According Shadlou and Battacharya [37] all piles tested are flexible. The soil stiffness for flexible piles were calculated using the approach proposed by Pentre [1], although that proposed by Shadlou and Battacharya [37] could also be used, the effect on f_n being negligible.

The Darvishi-Alamouti et al. [42] method used the Poulos & Davis [46] to define the limit for pile behaviour between slender and rigid:

$$L_P/T \leq 2 \quad \text{rigid pile} \tag{22}$$

$$L_P/T \geq 4 \quad \text{slender pile} \tag{23}$$

where:

$$T = \left(\frac{EI}{n_h}\right)^{0.25} \tag{24}$$

The 1 g models were divided into rigid (PL1L, PL4L, PL1D and PL4D), intermediate (PL2L, PL3L, PS1L, PS2L, PS4L, PL2D, PL3D, PS1D, PS4D) and slender (PS3L, PS2D, PS3D) piles. The 50 g prototype had a different classification having slender (PL1L, PL2L, PL4L, PS1L, PS2L, PS3L, PS4L, PL3D, PS1D, PS2D, PS3D, PS4D) and intermediate (PL3L, PL1D, PL2D and, PL4D) behaviour. The natural frequency of intermediate piles was linearly interpolated between rigid f_n and slender f_n calculated using the Darvishi-Alamouti et al. [42] solution.

A comparison of the calculated natural frequency considering SSI ($f_{n\text{-}TSSI}$) and the measured natural frequency (f_n) is presented in Fig. 18. This figure presents the centrifuge test (prototype scale) and the 1 g test (model scale) for the five proposed approaches.

The results of Arany et al. [36], Veletsos and Meek [43] and Gazetas [44] overestimate the experimentally measured natural frequency, but appear to do so by a predictable degree, all results falling onto a single trendline. The methodology of Kumar and Prakash [45], however, shows considerable scatter for the 1 g monopile test (Fig. 18a and c). It is clear that the tendency [36,43–45] is for the results to become better at low frequency as these solutions approach the fixed base condition. The real wind turbine structure presented less f_n than the experimental data, because the tower is higher. Therefore, the theoretical solution should present better results for practical applications.

The Darvishi-Alamouti et al. [42] method presented a linear trendline, but underestimated the measured values. However, adopting

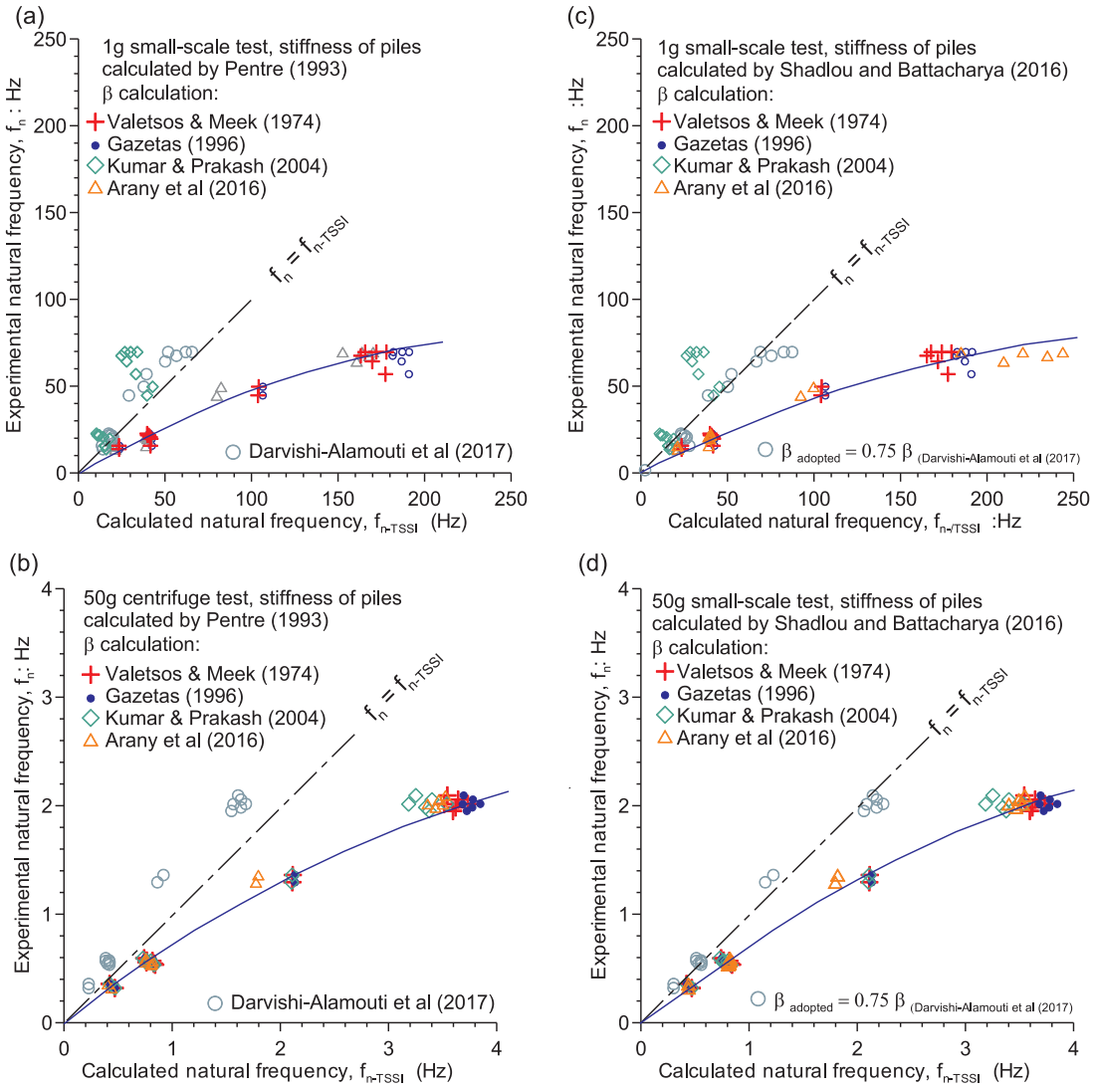

Fig. 18. Comparison of experimental results and theoretical values of natural frequency.

a factor $\beta = 0.75$ multiplying the frequency calculated by Darvishi-Alamouti et al. [42] gives an excellent prediction of the experimental results (Fig. 18c and d).

The effect of soil densification due to vibration (increasing f_n) and cyclic loading (decreasing f_n) should influence the soil stiffness especial in the real structure. As the forces applied were very low the present tests these effects are less important and the effects were not be taken into account.

9. Conclusion

This paper presented a methodology to measure the natural frequency of monopiles in centrifuge tests for loose and dense sand in well-controlled conditions and compared the results with theoretical solutions. The experimental results show that the fixity provided by the pile has a large effect on the natural frequency of the system, although for many geometries tested here the length of the piles was sufficient that increasing pile length had only a modest effect on the natural frequency. The frequencies observed were, however, lower than those of the fixed base structure, a point of fixity existing beneath the soil surface leading to an increased cantilever length and thus a reduced natural frequency.

The ratio of free length and embedded depth (L_T/L_P) was also investigated. Only two different free lengths were used, and it is clear that the natural frequency changes inversely to the free length. For the same free length (L_P = 10 m), the natural frequency and $f_n/f_{n\text{-str}}$ increase when the embedded depth increases (or L_T/L_P decreases). Although the relative densities of the two sand samples are very different, the data show only small differences in the natural frequency obtained, possibly due to the conflicting effects of increased stiffness but also increased added mass from the participating soil.

Small-scale tests under 1 g conditions were also performed using the same models, sand conditions, and other variables. When comparing the response, the low stress level of the 1 g tests reduced the soil stiffness while the pile stiffness was maintained. The experimentally observed dynamic response illustrates this difference with the f_n measured in the centrifuge scale model being higher than that 1 g, the variation not being a constant or following a well-established correlation.

Acknowledgments

The authors would like to thank the Brazilian National Council for Scientific and Technological Development (CNPq 405759/2013-4), the São Paulo Research Foundation (FAPESP - 2015/10223-2), the Schofield Centre and the University of Cambridge for logistical and financial support.

References

[1] Pender M. Aseismic pile foundation design analysis. Bull N Z Natl Soc Earthq Eng 1993;26:49–160.
[2] Hardin BO, Drnevich VP. Shear modulus and damping in soils: design equations and curves. J Soil Mech Found Div 1972;98:667–92.
[3] Wiser R, Jenni K, Seel J, Baker E, Hand M, Lantz E, et al. Expert elicitation survey on future wind energy costs. Nat Energy 2016;1:16135.
[4] European Wind Energy Association. The European offshore wind industry-key trends and statistics 2016. A report by the European Wind Energy Association. E.W.E. Association; 〈http://www.ewea.org〉 [Accessed 8 September 2017]; 2017.
[5] Smith A, Stehly T, Musial W. 2014–2015 Offshore wind technology market report. USA: NREL; 2015.
[6] LeBlanc C, Houlsby GT, Byrne BW. Response of stiff piles in sand to long-term cyclic lateral loading. Géotechnique 2010;60:79–90.
[7] Bisoi S, Haldar S. Dynamic analysis of offshore wind turbine in clay considering soil–monopile–tower interaction. Soil Dyn Earthq Eng 2014;63:19–35.
[8] Byrne BW, Houlsby GT. Foundations for offshore wind turbines. Philos Trans A Math Phys Eng Sci 2003;361:2909–30.
[9] Arany L, Bhattacharya S, Macdonald J, Hogan SJ. Simplified critical mudline bending moment spectra ofoffshore wind turbine support structures. Wind Energy 2015;18:2171–97.
[10] LeBlanc C. Design of offshore wind turbine support structures: selected topics in the field of geotechnical engineering [Ph.D. thesis]. Aalborg University; 2009.
[11] Hasselmann K, Barnett TP, Bouws E, Carlson H, Cartwright DE, Enke K, et al. Measurements of wind-wave growth and swell decay during the Joint North Sea Wave Project (JONSWAP). Ergänzungsheft zur deutschen hydrographischen zeitschrift reiche A 12. Hamburg: D.H. Institut; 1973.
[12] DNV (Det Norske Veritas). Guidelines for design of wind turbines. 2nd ed Denmark: Wind Energy Department, Risø National Laboratory; 2002.
[13] Zaaijer MB. Foundation modelling to assess dynamic behaviour of offshore wind turbines. Appl Ocean Res 2006;28:45–57.
[14] Alexander NA. Estimating the nonlinear resonant frequency of a single pile in nonlinear soil. J Sound Vib 2010;329:1137–53.
[15] Arany L, Bhattacharya S, Hogan SJ, Macdonald J. Dynamic soil-structure interaction issues of offshore wind turbines. Proceedings of the 9th International Conference on Structural Dynamics, Portugal: EURODYN; 2014.
[16] Bhattacharya S, Nikitas N, Garnsey J, Alexander NA, Cox J, Lombardi D, et al. Observed dynamic soil–structure interaction in scale testing of offshore wind turbine foundations. Soil Dyn Earthq Eng 2013;54:47–60.
[17] Prendergast LJ, Gavin K, Doherty P. An investigation into the effect of scour on the natural frequency of an offshore wind turbine. Ocean Eng 2015;101:1–11.
[18] Burd HJ, Byrne BW, McAdam R, Houlsby GT, Martin CM, Beuckelaers WJAP, Zdravković L, Taborda DMG, Potts DM, Jardine RJ, Gavin K, Doherty P, Igoe D, Skov Gretlund J, Pacheco Andrade M. Wood, A. M.r Design aspects for monopile foundations. In: Proceedings TC 209 workshop on foundation design for offshore wind structures, 19th ICSMGE, Seoul, 3-44; 2017.
[19] Tan FSC. Centrifuge and theoretical modelling of conical footing on sand [Ph.D. thesis]. University of Cambridge; 1990.
[20] Mitrani H. Liquefaction remediation techniques for existing buildings [Ph.D. thesis]. University of Cambridge; 2006.
[21] Heron CM. The dynamic soil structure interaction of shallow foundation on dry sand beds [Ph.D. thesis]. University of Cambridge; 2013.
[22] Kirkwood P. Cyclic lateral loading of monopile foundations in sand [Ph.D. thesis]. University of Cambridge; 2015.
[23] Madabhushi SPG, Houghton NE, Haigh SK. A new automatic sand pourer for model preparation at University of Cambridge. In: Proceedings of the 6th international conference on physical modelling in geotechnics. Hong Kong: Taylor & Francis; 2006 Aug 4-6.
[24] Ghosh B, Madabhushi SPG. An efficient tool for measuring shear wave velocity in the centrifuge. In: Proceedings of the international conference on physical modelling in geotechnics, 119-124; 2002.
[25] Madabhushi G. Centrifuge modelling for civil engineers. Boca Raton: CRC Press; 2014.
[26] Schofield. Cambridge geotechnical centrifuge operations. Géotechnique 1980 1980;25:743–61.
[27] Technologies Cedrat. Technical specification of Amplified Piezoelectric Actuator - APA400MML, Cedrat technologies and innovation in mechanics . 〈http://www.cedrat-technologies.com〉 [Accessed 7 February 2017]; 2015.
[28] Cabrera M, Caicedo B, Thorel L. Dynamic actuator for centrifuge modeling of soil-structure interaction. Geotech Test J 2012;35:1–9.
[29] Seed HB, Idriss IM. Soil modules and damping factors for dynamic response analyses. Berkeley, CA: University of California, Earthquake Engineering Research Center; 1970. [Report No. EERC 70-10].
[30] Oztoprak S, Bolton MD. Stiffness of sands through a laboratory test database. Géotechnique 2013;63:54–70.
[31] Hardin BO, Black WL. Sand stiffness under various triaxial stresses. J Soil Mech Found Div ASCE 1966;92(No. SM2):667–92.
[32] Randolph MF. The response of flexible piles to lateral loading. Géotechnique 1981;31:247–59.
[33] Novak M, El Sharnouby B. Stiffness constants of single piles. J Geotech Eng 1983;109:961–74.
[34] Carter JP, Kulhawy FH. Analysis of laterally loaded shafts in rock. J Geotech Eng 1992;118:839–55.
[35] Higgins W, Vasquez C, Basu D, Griffiths DV. Elastic solutions for laterally loaded piles. J Geotech Geoenviron Eng 2013;139:1096–103.
[36] Arany L, Bhattacharya S, Macdonald JHG, Hogan SJ. Closed form solution of Eigen frequency of monopile supported offshore wind turbines in deeper waters incorporating stiffness of substructure and SSI. Soil Dyn Earthq Eng 2016;83:18–32.
[37] Shadlou M, Bhattacharya S. Dynamic stiffness of monopiles supporting offshore wind turbine generators. Soil Dyn Earthq Eng 2016;88:15–32.
[38] Jalbi S, Shadlou M, Bhattachary S. Impedance functions for rigid skirted caissons supporting offshore wind turbines. Ocean Eng 2017;150:21–35.
[39] Arany L, Bhattacharya S, MacDonald J, Hogan SJ. Design of monopiles for offshore wind turbines in 10 steps. Soil Dynam Earthq Eng 2017;92:126–52.
[40] Vesic AB. Bending of beams resting on isotropic solid. J Eng Mech Division 1961:35–64.
[41] van der Tempel J, Molenaar DP. Wind turbine structural dynamics-a review of the principles for modern power generation, onshore and offshore. Wind Eng 2002;26:211–20.
[42] Darvishi-Alamouti S, Bahaari M, Moradi M. Natural frequency of offshore wind turbines on rigid and flexible monopiles in cohesionless soils with linear stiffness distribution. Appl Ocean Res 2017;92:91–102.
[43] Veletsos AS, Meek JW. Dynamic behaviour of building-foundation systems. Earthq Eng Struct Dyn 1974;3:121–38.
[44] Gazetas G. Soil dynamics and earthquake engineering-case studies. Athens: Simeon Publications (in Greek); 1996.
[45] Kumar S, Prakash S. Estimation of fundamental period for structures supported on pile foundations. Geotech Geol Eng 2004;22:375–89.
[46] Poulos H, Davis E. Pile foundation analysis and design. New York: Rainbow Bridge Book Co., Wiley; 1980.